



# Heat Transport Pathways into the Arctic and their Connections to Surface Air Temperatures

Daniel Mewes<sup>1</sup> and Christoph Jacobi<sup>1</sup>

<sup>1</sup>Leipzig Institute for Meteorology, University of Leipzig

**Correspondence:** Daniel Mewes ([daniel.mewes@uni-leipzig.de](mailto:daniel.mewes@uni-leipzig.de))

**Abstract.** Arctic Amplification causes the meridional temperature gradient between middle and high latitudes to decrease. It is assumed that through this decrease the large-scale circulation changes and therefore the meridional transport of heat and moisture increases. This in turn may increase Arctic warming even further. To investigate patterns of Arctic temperature, horizontal fluxes and their changes in time, we analyzed ERA-Interim daily winter data of vertically integrated horizontal heat transport using Self-Organizing Maps (SOM). Three general transport pathways have been identified: the North Atlantic Pathway with transport mainly over the northern Atlantic, the North Pacific Pathway with transport from the Pacific region, and the Siberian Pathway with transport towards the Arctic over the eastern Siberian region. Transports that originate from the North Pacific are connected with negative temperature anomalies over the central Arctic. These North Pacific Pathways are getting less frequent during the last decades. Patterns with origin of transport in Siberia are found to have no trend and show cold temperature anomalies north of Svalbard. It was found that transport patterns that favor transport through the North Atlantic into the central Arctic are connected with positive temperature anomalies over large regions of the Arctic. These temperature anomalies resemble the warm Arctic cold continents pattern. Further, it could be shown that transports through the North Atlantic are getting significantly more frequent during the last decades.

## 1 Introduction

The Arctic regions play a significant and specific role in climate change. The temperature increases much faster compared to the rest of the globe (Stroeve et al., 2012; Wendisch et al., 2017), which is called Arctic Amplification. This effect leads, e.g., to a particularly rapidly decreasing sea ice cover.

Following these changes in temperature and sea ice cover it was found that the sea level pressure (SLP) decreases over the Arctic in the winter season (Gillett et al., 2003; Screen et al., 2014). This itself might alter the circulation and thus the transport of air masses into and out of the Arctic. Analyses of the decadal variability in EC-Earth model (Hazeleger et al., 2012) runs showed that in a warmer climate the Aleutian Low intensifies during winter months, which changes the circulation patterns (Linden et al., 2017). The decrease of the temperature difference between the Arctic and mid latitudes due to Arctic Amplification is suggested to be followed by a change in the meridional transport of heat into the Arctic, which has been seen in reanalysis data (Graversen, 2006; Vinogradova, 2007). Analysis of regional climate model output has shown that at the end of the 21st century the seasonal mean layer thickness between 1000 and 300 hPa over the Arctic will likely increase



significantly, while the interannual variability increases (Rinke and Dethloff, 2008). To summarize, there is clear indication that Arctic Amplification alters the circulation and heat transport patterns in the Arctic.

To understand how circulation and transport are connected to other meteorological variables, the Self-Organizing Map (SOM) method has been shown to be a viable cluster and pattern extraction tool (Liu et al., 2006; Liu and Weisberg, 2011).

- 5 Cassano et al. (2006) evaluated model representations and projections of the SLP patterns over the Arctic. Corresponding temperature and precipitation anomalies have been attributed to the respective patterns that have been emerged from SOM analyses. They found that SLP patterns that feature an extended North Atlantic storm track and a strong Aleuten low are connected with positive temperature anomalies. Negative precipitation anomalies over the North Atlantic were found for SLP pattern with generally strong high SLP. Skific et al. (2009) used SOM analyses to validate performance of the Community  
10 Climate System Model. They showed that the model successfully captures major SLP patterns, which has been derived by the SOM from ERA-40 data. Additionally, they found through relating moisture transports to particular circulation regimes that by the late 21st century the transport is projected to be increased within the CCSM3. The SOM method was also used by Higgins and Cassano (2009) to determine the influence of reduced sea ice on the geopotential height of 1000 hPa over the Arctic using the CAM3 (Collins et al., 2006). They found that with reduced sea ice the geopotential height of 1000 hPa increases over  
15 Siberia, the Greenland and Norwegian Seas.

Lynch et al. (2016) used the SOM method to evaluate the connection between SLP patterns and the connection with high and low sea ice cover in the Pacific sector. They showed that years with low ice fraction are connected with positive temperature anomalies and transport originating from the south, while years with high ice concentration are connected with transport of ice from regions in the north even though the ice itself is melting.

- 20 Mattingly et al. (2016) have analyzed the tropospheric meridional moisture transport over Greenland using the SOM method and found that from 2000 to 2015 positive moisture transport anomaly patterns towards Greenland were more common compared to 1979 to 1994 and thus might have increased the melting of the Greenland ice sheet.

- The question remains to which degree different heat transport pathways into the Arctic are responsible for the increased Arctic warming. In this study we therefore focus on the general heat transport pathways into the Arctic in the winter months  
25 and on the corresponding temperatures over the Arctic by using the SOM method. Winter was chosen as the Arctic temperature is most sensitive to influences through transports in this season (Yoshimori et al., 2017). We use ERA-Interim reanalyses (Dee et al., 2011; ECMWF, 2017) for clustering the vertically integrated horizontal heat transport. This is used to obtain informations from the whole tropospheric column. Further, the temporal evolution of occurrence frequencies for the obtained patterns is analyzed, as well as corresponding temperature anomalies for the Arctic region. In Sect. 2 the used data and SOM method are  
30 presented. The results are found in Sect. 3, and are followed by a discussion in Sect. 4. Section 5 concludes the paper.



## 2 Method and data

### 2.1 Data

In this study daily mean ERA-Interim (Dee et al., 2011) data were analyzed for the winter months (December to February) from 1979 to 2016. Data were provided at a horizontal grid resolution of  $0.75^\circ \times 0.75^\circ$  with 37 vertical levels by ECMWF (2017). ERA Interim was chosen as it represents the temperature in the Arctic well (Chaudhuri et al., 2014; Simmons and Paul, 2015). Daily means were calculated from 6-hourly output. The vertically integrated daily horizontal heat transport  $Q$  is calculated at each grid point as follows:

$$Q = \frac{1}{g} \int_{1000 \text{ hPa}}^{200 \text{ hPa}} v(p) c_p T(p) dp. \quad (1)$$

Here,  $g$  is the gravitational acceleration (taken as  $9.81 \text{ m/s}^2$ ),  $v$  is the horizontal wind vector,  $c_p$  is the specific heat constant at constant pressure,  $T$  is the temperature and  $p$  is the pressure. The integration limits of 1000 hPa and 200 hPa were chosen to obtain an average picture over the Arctic troposphere.

### 2.2 Self-Organizing Maps

The SOM is an artificial neural network developed by Kohonen (1998), and it is used to reduce the dimensionality of a data set by organizing it in a two-dimensional array, called map. SOMs were created by using the python package “somoclu” (Wittek et al., 2017). The SOM was used to analyze the tropospheric horizontal heat transport calculated from ERA-Interim. The SOM clustering is used to find common transport features in the Arctic. Further, the two meter air temperature anomalies corresponding to the clustering of the tropospheric horizontal heat transport are analyzed. This is done to obtain the respective transport effect on the temperature depending on the different transport features. A SOM with the size of 4 columns  $\times$  3 rows was chosen for our analysis of transport into the Arctic Ocean; it provided the best balance of generalization without losing too many distinct states. In addition to the clustering of the SOM itself, we chose to group similar transport patterns manually. This is commonly done in the literature (e.g. Mattingly et al., 2016; Higgins and Cassano, 2009).

## 3 Results

### 3.1 Heat transport SOM

The SOM of the vertically integrated heat transport is shown in Fig. 1. Each pattern features different transport strengths and directions as shown by the vectors. For a view on the general transport pathways we decided to further gather the patterns into three groups chosen according to the transport from middle latitudes into the central Arctic (north of  $80^\circ \text{ N}$ ). This manual grouping leads to a more transparent view on the actual clustering of the data.

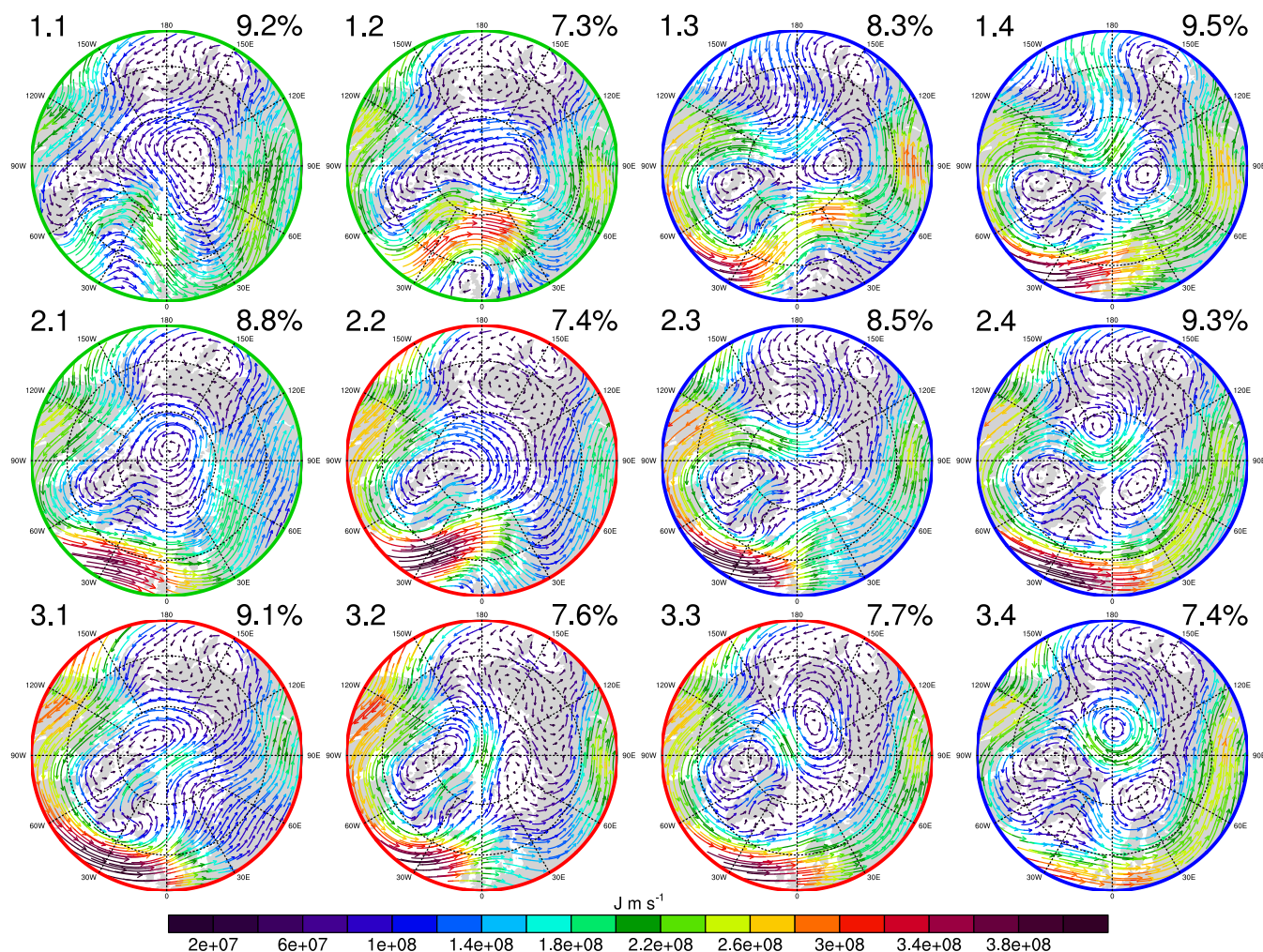


**Figure 1.** 4×3 SOM of vertically integrated (200 hPa -1000 hPa) horizontal heat transport from winter ERA-INTERIM data (1979-2016). Numbers on the top left are used to name different patterns, percentages in the top right of each pattern correspond to the relative frequency of occurrence during the analyzed time period. The maps are centered at 0°E. Red vectors correspond to stronger transports, while blue vectors correspond to weaker transports. Differently colored frames indicate patterns that were grouped together.

The composite transports are shown in Fig. 2. They were derived by adding the distinct patterns of each group in Fig. 1 weighted by their relative frequency of occurrence. Subsequently, we will call them the North Atlantic Pathway, the Siberian Pathway, and the North Pacific Pathway.

The red framed patterns in Fig. 1 and 2 show the North Atlantic Pathway. Corresponding patterns for the North Atlantic Pathway are patterns 2.2, 3.1, 3.2, 3.3. These patterns share a heat transport that is going from North Atlantic either over  
 5 Pathway are patterns 2.2, 3.1, 3.2, 3.3. These patterns share a heat transport that is going from North Atlantic either over Greenland or through the Fram Strait and over Svalbard into the central Arctic.



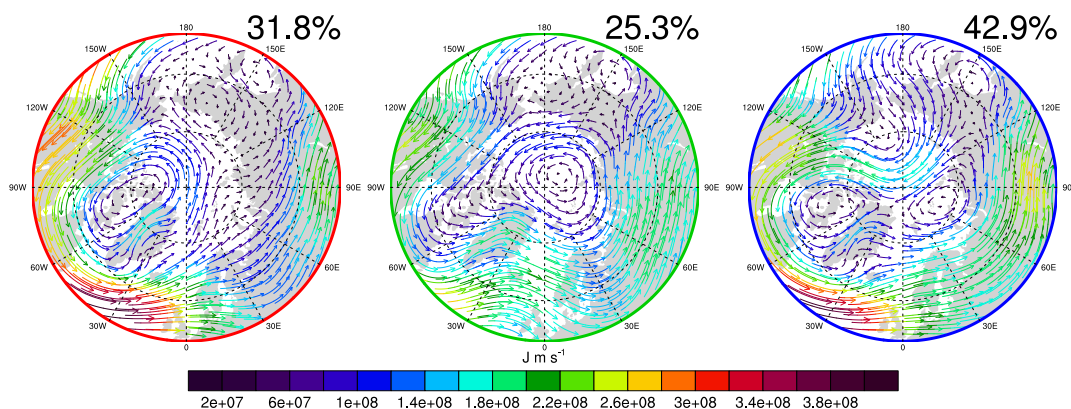


**Figure 2.** The three different transport pathways: the North Atlantic Pathway (left; red colored frame), the Siberian Pathway (middle; green colored frame), and the North Pacific Pathway (right; blue colored frame), derived by the composites of the selected patterns of Fig. 1 weighted by their relative frequency of occurrence within the group.

Patterns with a green frame correspond to transport that originates from central Siberia or northern Siberia and is directed into the central Arctic by a cyclone motion with its center over the Kara Sea, Laptev Sea, or the North Pole. These features are summarized as the Siberian Pathway. The Siberian Pathway consists of the patterns 1.1, 1.2, and 2.1. The transport structure of Pattern 2.1 is mainly zonally within the central Arctic, and no strong meridional transport is present. However, its general structure with a centralized center of cyclonic motion fits best into the Siberian Pathway group.

The North Pacific Pathway (blue frames) arises from the patterns 1.3, 1.4, 2.3, 2.4, and 3.4. The main transport occurs from the North Pacific through east Siberia into the central Arctic. This occurs mostly with two cyclone motions with one center at the Barents Sea or Laptev Sea and the other center over the Northwest Passage. In some cases (see patterns 3.4, 2.3, and 2.4) an anti-cyclone motion with the center north of the Bering Strait or within the central Arctic is present.

### 3.2 Temperature anomaly composites according to transport pathways

Figure 3 shows the composites of the temperature anomalies corresponding to the respective pathways. The red framed plot shows the anomalies related to the North Atlantic Pathway, the green one those related to the Siberian Pathway, and the blue one those related to the North Pacific Pathway. The North Atlantic Pathway related temperature anomalies (left panel Fig. 3) show increased temperature from the North Atlantic into the central Arctic with a maximum of 7 K north of Svalbard. For northern Canada, the Bering Strait and central Siberia a cold anomaly is observed with a minimum of  $-3.5$  K at the Bering Strait and north of Lake Baikal. The negative anomaly in Siberia results from the increased transport over the North Atlantic, which results in a decrease of zonal transport of heat to Siberia, and in an increase of transport of cold air from the north.

The Siberian Pathway (middle panel Fig. 3) is connected with higher temperatures over Siberia, as well as with warm anomalies over Northern America and Greenland with temperature anomalies as high as 5.5 K at the southern tip of Greenland. Negative temperature anomalies occur over Northern Europe, through the Fram Strait and Svalbard into the central Arctic, the

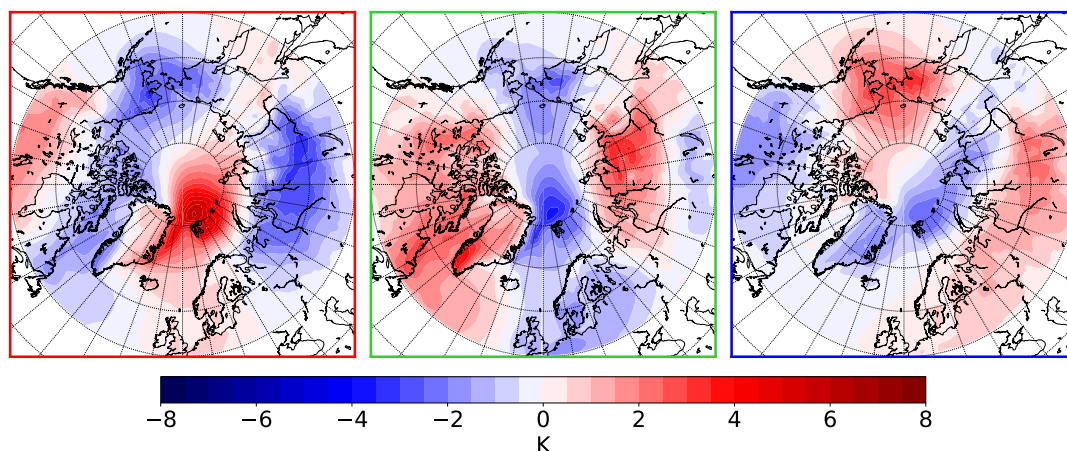


**Figure 3.** Composite of 2 meter temperature anomalies for each of the three pathways: the North Atlantic Pathway (left; red colored frame), the Siberian Pathway (middle; green colored frame), and the Northern Pacific Pathway (right; blue colored frame). Contour spacings show temperature anomalies in 0.5 K. Blue colors indicate a cold anomaly and red colors indicate a warm anomaly compared to the mean of the analyzed time frame.

Chukchi Sea, and the Bering Strait, with anomalies as low as  $-4$  K north of Svalbard. This temperature pattern occurs because of the limited heat transport through the North Atlantic and the more zonally favored transport over Europe and Siberia.

The North Pacific Pathway (right panel of Fig. 3) composite shows increased temperature over large parts of Eurasia connected with zonal transport over the continent. Positive temperature anomalies are also seen over the Bering Strait, and the Chukchi Sea (up to 3.5 K), together with northward transport there (right panel of Fig. 2). From North America over Greenland and Svalbard to the Laptev Sea a cooling effect is observed, with the maximum of  $-2.5$  K west of Svalbard.

### 3.3 Meridional heat transport

In order to more clearly show the transport of heat into the Arctic through the three identified patterns, we analyzed the longitudinal distribution of the meridional heat flux. To this end, for each of the three pathways the mean meridional flux of heat  $H = v c_p T$ , with  $v$  as the meridional wind component, was calculated from all winter days during those the respective pattern was the dominating one. Again  $H$  was integrated over 1000 to 200 hPa.

The mean of the meridional transport at  $75^\circ$  N is shown in Fig. 4. Its standard deviation has a similar order of magnitude than the total atmospheric energy transport at  $60^\circ$  N presented by Graversen (2006, Fig. 4 b). The zonal mean long-term mean transport of  $H$  amounts to 1.66 GW.

Figure 5 shows the meridional heat transport anomalies at  $75^\circ$  N at each longitude grouped into the three transport pathways. Note that the standard deviation is in the order of 0.2 PW due to the used daily data of the corresponding group that is highly variable. For the composite of the North Atlantic Pathway (red, left panel) we have maximum positive anomalies of the meridional heat transport from  $50^\circ$  W to  $50^\circ$  E, and negative anomalies from  $60^\circ$  E to  $140^\circ$  W. The North Pacific Pathway

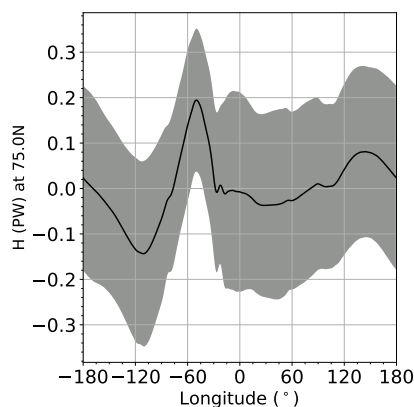


**Figure 4.** Mean vertically integrated (200 hPa–1000 hPa) meridional heat transport at 75° N given in Petawatts. Grey shaded areas show the standard deviation.

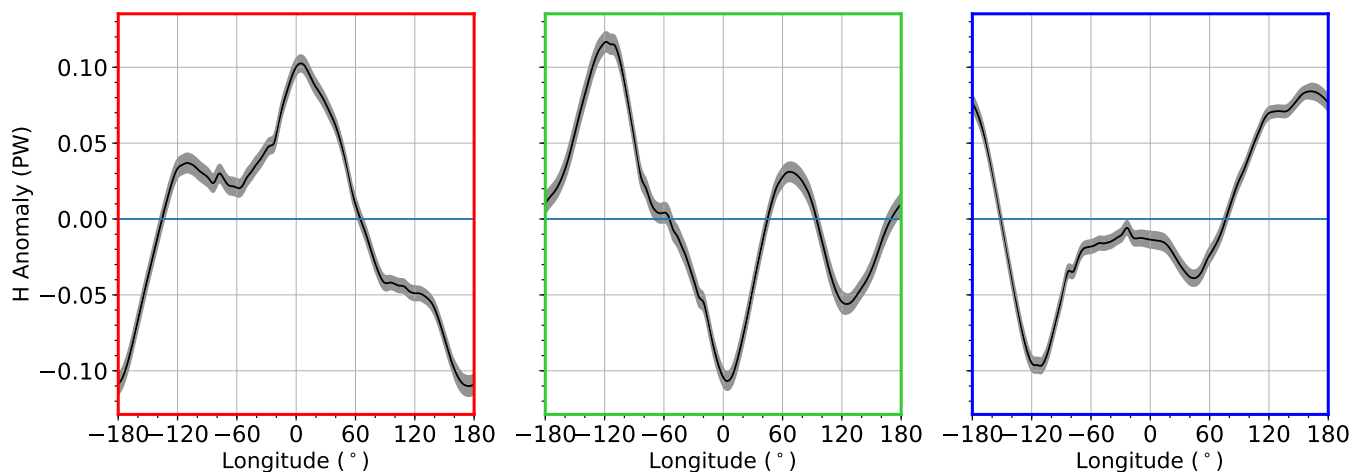


**Figure 5.** Composite of meridional heat transport anomalies at 75° N given in PW for each of the three pathways. Red frame means transports through the North Atlantic, green frame through Siberia, and blue frame transports through the North Pacific. Grey shaded areas show the standard error. Positive sign denotes a transport anomaly to the north and negative sign denotes a transport anomaly to the south.

(blue, right panel) is connected with positive transport anomalies from 80° E to 170° W. This corresponds to the described pathway: originating from the North Pacific and going over Eastern Russia to the central Arctic. The Siberian Pathway (green, middle panel) shows positive anomalies from 180° W to 60° W and from 30° E to 100° E. Generally, the meridional transports of the three groups fit well to the described pathways.



### 3.4 Trend of transport pathways

Overall, the North Atlantic pathway occur during about 32 %, the North Pacific pathway during about 43 %, and the Siberian Pathway during about 25 % of the analyzed time period. For each of the three groups the relative frequency of occurrence was calculated for each winter and the respective time series are shown in Fig. 6. The positive trend of the frequency of occurrence

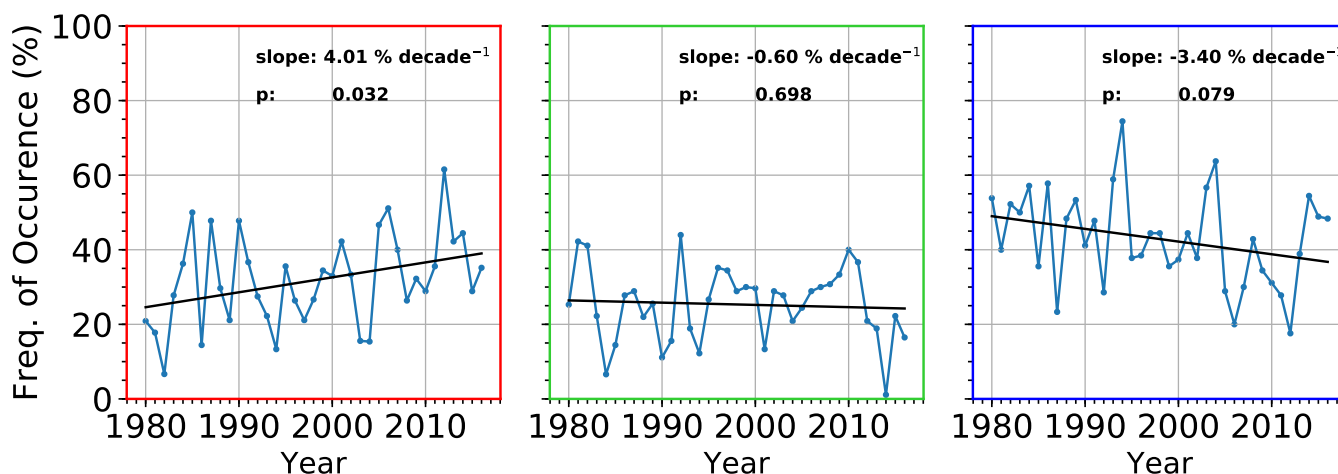


**Figure 6.** Frequency of occurrence for each transport pathway group according to the coloring (Fig. 1). The blue line shows the frequency of occurrence for each years winter from 1979 to 2015. The black line shows the linear trend line. p values are shown according to a 2 sided t-test.

- 5 for the North Atlantic Pathway (left panel) is significant at the 95 % confidence level with a increase of 4 % per decade. The group of the Siberian Pathway (middle panel) does not provide a significant trend of the frequency of occurrence (0.6 % per decade). A significant negative trend at the 90 % confidence interval was found for the North Pacific Pathway (right panel) with a decrease of -3.4 % per decade.

### 3.5 Temperature trends

- 10 Comparing the general temperature trend with the resulting temperature anomalies due to different transport pathways indicates to which degree heat transports might play a role for the warming of the Arctic. The general temperature trend for the winter season during the analyzed time period is shown in the left panel of Fig. 7. Generally it can be seen that the trend exceeds 3.5 K decade<sup>-1</sup> for the region east of Svalbard. Positive trends are significant for large regions of the Barents Sea, the Kara Sea, the Laptev Sea, the Arctic Ocean north of Russia, and the Baffin Bay. Significant negative temperature trends occur over  
15 Siberia, but only for very small regions.

To calculate the influence of changes in transport pathways we calculated the weighted average of the temperature anomaly of the North Atlantic Pathway and the inverse temperature anomaly of the North Pacific Pathway (right panel of Fig. 7). This was done to take into account the influence of an increased occurrence frequency of the North Pacific Pathway and a decrease



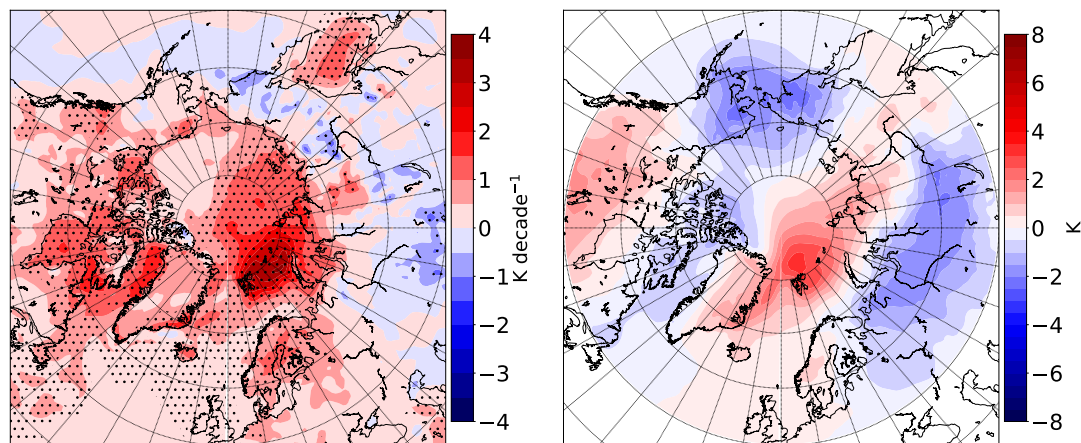


**Figure 7.** Left panel: temperature trend for the winter mean. Calculated for the winters from 1979/80 to 2015/16. Dotted regions indicate significance at the 95 % level. Trend is given in Kelvin per decade. Right panel: composite of temperature anomalies from the North Atlantic Pathway and the North Pacific Pathway in Fig. 3, weighted by their relative frequency of occurrence (Fig. 2 top right number).

of occurrence frequency for the North Pacific Pathway, and thus to analyze the possible change in temperature according to a trend in the transport pathways. Each of the temperature anomaly fields were weighted by the relative frequency of occurrence shown in Fig. 2. The Siberian Pathway was not included as it does not show a trend in the occurrence frequency. This new composite shows similar features compared to the temperature anomaly of the North Atlantic Pathway (Fig. 3 left panel), which is owing to the fact that the temperature anomalies connected to the North Atlantic and North Pacific Pathways are broadly inverse to each other.

The regions of large temperature anomalies are more confined and weaker than the ones considering single pathways alone. The largest positive temperature anomaly occurs north of Svalbard with up to 3.5 K. Negative anomalies occur over the Bering Strait (-3.0 K) and north of Lake Baikal (-2.5 K).

The winter temperature trend shows a strong positive signal east of Svalbard. This signal can partly be seen in the temperature anomaly which also shows a positive signal in this region. For the regions that correspond to lower temperatures with an increased occurrence of the North Atlantic Pathway and a decreased occurrence of the North Pacific Pathway no significant temperature trend can be found on the left panel of Fig. 7. This suggests that the temperature anomalies due to the transport changes are counteracted by other processes. It has to be noted, that the heat transport cannot be accounted for changes in the temperature anomalies alone. Other transports and processes affect the temperature as well, even to a higher degree.

#### 4 Discussion

The change of influence and connection of atmospheric circulation with surface temperature is a highly discussed topic, especially in terms of the increased temperature rise in the Arctic. Here we grouped data according to distinct pathways based on SOM analysis and looked at related temperatures and the respective trend of the pathways.



The increase in frequency of transports through the Northern Atlantic, as shown for the North Atlantic Pathway, has also been found by Dahlke and Maturilli (2017). They analyzed the transports of air masses to the region of Ny-Alesund using backward trajectories. They were able to find a more frequent source region of air masses in the North Atlantic, while we could show that and the transport through the North Atlantic is getting more frequent. Dahlke and Maturilli (2017) identified a positive temperature anomaly over the Svalbard region that is connected with changes in advection of air masses. We find that the increased frequency of the North Atlantic Pathway is connected with temperature anomalies that favors a strongly positive anomaly in the central Arctic and strongly negative anomalies over Siberia and the Bering Strait. This is following from the transport of heat to the northern regions instead of transport to Siberia.

The temperature composite from the North Atlantic Pathway has also similar features compared to the cold continents and warm Arctic proposed by Overland et al. (2011). In our analysis negative temperatures anomalies over Canada are not seen. But the cold anomalies over central Siberia, as well as the warm anomaly sector over the central Arctic are quite well reproduced for transports through the North Atlantic.

Adams et al. (2000) found transport of heat from the North Atlantic and North Pacific to the Arctic for transient and stationary eddies. Also Messori et al. (2018) found a systematic transport of moisture through the Atlantic sector into the Arctic for warm spells. These warm spells are accompanied by advection of cold air across Siberia, which can be partly seen in the temperature composite of our the North Atlantic Pathway. The transports into the Arctic discussed by Messori et al. (2018) are comparable with the transports shown in our results. The general trend of increased northward transport of air can also be seen in regional analysis by Mattingly et al. (2016). They focused on the moisture transport over Greenland. Their analysis shows an increase of moist states over Greenland, which are partly connected with more northward transports. Rinke et al. (2017) analyzed extreme cyclone events in the Arctic wintertime from measurement at Ny-Alesund and from ERA-Interim reanalyses. They found that the number of extreme cyclone events increases. For days with extreme cyclone events at Ny-Alesund their temperature anomaly pattern looks similar as the temperature pattern shown in the North Atlantic sector for the North Atlantic Pathway. This suggests that the origin of the extreme cyclones analyzed in Rinke et al. (2017) might be connected with increased transport through the North Atlantic sector to Svalbard.

We focused on an tropospheric column information of heat transport compared to the analysed SLP in Cassano et al. (2006). For the winter months, they were able to connect SLP patterns with lower pressure over the Bering Strait and the North Atlantic and higher pressure over Siberia with a temperature anomaly that shares very similar features to those of the North Atlantic Pathway found in the presented work here.

The frequency of occurrence of the North Pacific Pathway decreases during the last decades. This is connected with less frequent negative temperature anomalies over the central Arctic. For the winter Matthes et al. (2015) show that the number of cold spell events is decreasing over Scandinavia and Northern Canada, while for Siberia also regions with a increase of cold spells could be found. Warm spells showed strong significant increase over Scandinavia. Matthes et al. (2015) analyzed the trends for warm and cold spells over the land masses and islands in the Arctic using daily station data and ERA-Interim reanalysis. Looking at the trend of regional temperature extremes at Ny-Alesund, Wei et al. (2015) could show that cold extremes have a negative trend and warm extremes have a positive trend. These results agree with the connection of the North



Pacific Pathway (North Atlantic Pathway) to cold (warm) temperature anomalies and a decrease (increase) in frequency of occurrence.

We compared the resulting mean temperature anomalies for the generally change in transport – decrease of occurrence frequency of North Pacific Pathway and increase of occurrence frequency of North Atlantic Pathway – with the general temperature trend for the winter season from 1979/80 to 2015/16. We found trends over  $3.5 \text{ K decade}^{-1}$  for the general temperature trend in winter west of Svalbard. Graversen (2006) analyzed the influence of the atmospheric northward energy transport on the surface air temperature for ERA-40 reanalysis for the years 1958 to 2001. He found that the atmospheric northward energy transport addresses about  $0.15 \text{ K decade}^{-1}$  over Svalbard. Compared to our analyzed time frame this would add up to about 0.6 K anomaly over Svalbard. We identified a positive temperature anomaly of about 3.0 K over Svalbard, which is about 2.4 K more than explained by the total atmospheric northward energy transport. Due to finding connected temperature fields for distinct transport pathways, we are able to see all influences of the atmosphere under these specific pathways and not only the specific influence of the northward energy transport, which was analyzed by Graversen (2006).

It was found that at regions where the change in transport will favor negative temperature anomalies (Siberia and Bering Strait) no significant trend in temperature is present. For regions north and east of Svalbard the change in transport is connected with positive temperature anomalies that also coincide with regions of positive trends in temperature. Comparing the combined composite of temperature anomalies connected to the changing of the major transport pathways (right panel of Fig. 7) to the temperature anomalies of the Siberian Pathway (Fig. 3 middle panel) shows that in general the central Arctic tends to become warmer while the Bering Strait tends to become cooler in relation to the change in transport. So in general, the change of transports would lead to more frequent negative temperature anomalies over the Bering Strait and Siberia. These cannot be seen in the trends shown on the left panel of Fig. 7. This demonstrates that the surface temperature trend cannot be explained by the transport pathway connected temperature anomalies alone. Therefore the variability of the Siberian Pathway and the temperature anomalies connected to this have also be taken into account for the whole picture. But our results show the expected geographic distribution of surface temperature anomalies that coincides with these changes in the transport. These results are also a good example that the surface trend is influenced by a lot of processes and cannot be discussed solely by heat transport alone.

## 5 Summary and conclusion

With the SOM method we were able to find intrinsic heat transport patterns within the heat transport fields and used them as an guide for our analysis. Three distinct transport pathways were extracted from the SOM analysis: the North Atlantic Pathway, the Siberian Pathway, and the North Pacific Pathway. The North Atlantic Pathway is connected with transports through the North Atlantic into the Arctic, the North Pacific Pathway is connected with transports that originate from the North Pacific and enter the Arctic through east Siberia, and the Siberia Pathway is features by transports through the Arctic from central Siberia. We analyzed the temperature anomalies that are related to the different transport pathways. This type of analysis helps to get a more complete view of the atmosphere during these different transport pathways.



We conclude that during the last decades the transport through the North Atlantic into the Arctic has increased significantly. These North Atlantic Pathways are connected with positive temperature anomalies over the Arctic, and negative temperature anomalies over the Bering Strait and central Siberia. This shows that relating temperature anomalies based on the transport alone is favouring an increased pattern of warm Arctic and cold continents. Thus it can be stated that the warm Arctic and cold continents pattern is partly controlled by the increased northward heat transport through the North Atlantic.

A question that still remains open is the question of causality. To which degree the change in heat transports and circulation is changing the temperatures in a warming Arctic and to which degree is the temperature change influencing the heat transports and circulation themselves cannot be decided based on SOM analysis alone.

*Author contributions.* Daniel Mewes performed the data analysis and wrote the first draft of the manuscript. Christoph Jacobi initiated the project and made contributions to the results interpretation and manuscript writing.

*Competing interests.* The authors declare that they have no conflict of interest.

*Acknowledgements.* ERA-Interim reanalyses data have been provided by ECMWF [apps.ecmwf.int/datasets/data/](https://apps.ecmwf.int/datasets/data/). We gratefully acknowledge the support by the SFB/TR 172 “Arctic Amplification: Climate Relevant Atmospheric and Surface Processes, and Feedback Mechanisms (AC)<sup>3</sup>.” in the sub-project D01 funded by the DFG (Deutsche Forschungsgesellschaft). We thank Annette Rinke, AWI Potsdam, for helpful discussions and comments.



## References

- Adams, J. M., Bond, N. A., and Overland, J. E.: Regional variability of the Arctic heat budget in fall and winter, *J. Climate*, 13, 3500–3510, [https://doi.org/10.1175/1520-0442\(2000\)013<3500:RVOTAH>2.0.CO;2](https://doi.org/10.1175/1520-0442(2000)013<3500:RVOTAH>2.0.CO;2), 2000.
- Cassano, J. J., Petteri, U., and Amanda, L.: Changes in synoptic weather patterns in the polar regions in the twentieth and twenty-first centuries, part 1: Arctic, *International Journal of Climatology*, 26, 1027–1049, <https://doi.org/10.1002/joc.1306>, 2006.
- Chaudhuri, A. H., Ponte, R. M., and Nguyen, A. T.: A comparison of atmospheric reanalysis products for the Arctic Ocean and implications for uncertainties in air–sea fluxes, *Journal of Climate*, 27, 5411–5421, <https://doi.org/10.1175/JCLI-D-13-00424.1>, 2014.
- Collins, W. D., Rasch, P. J., Boville, B. A., Hack, J. J., McCaa, J. R., Williamson, D. L., Briegleb, B. P., Bitz, C. M., Lin, S.-J., and Zhang, M.: The Formulation and Atmospheric Simulation of the Community Atmosphere Model Version 3 (CAM3), *Journal of Climate*, 19, 2144–2161, <https://doi.org/10.1175/JCLI3760.1>, 2006.
- Dahlke, S. and Maturilli, M.: Contribution of atmospheric advection to the amplified winter warming in the arctic north atlantic Region, *Advances in Meteorology*, 2017, <https://doi.org/10.1155/2017/4928620>, 2017.
- Dee, D. P., Uppala, S. M., Simmons, A. J., Berrisford, P., Poli, P., Kobayashi, S., Andrae, U., Balmaseda, M. A., Balsamo, G., Bauer, P., Bechtold, P., Beljaars, A. C. M., van de Berg, L., Bidlot, J., Bormann, N., Delsol, C., Dragani, R., Fuentes, M., Geer, A. J., Haimberger, L., Healy, S. B., Hersbach, H., Hólm, E. V., Isaksen, I., Kållberg, P., Köhler, M., Matricardi, M., McNally, A. P., Monge-Sanz, B. M., Morcrette, J.-J., Park, B.-K., Peubey, C., de Rosnay, P., Tavolato, C., Thépaut, J.-N., and Vitart, F.: The ERA-Interim reanalysis: configuration and performance of the data assimilation system, *Quart. J. Roy. Meteor. Soc.*, 137, 553–597, <https://doi.org/10.1002/qj.828>, 2011.
- ECMWF: ERA interim, daily pressure levels. ECMWF, available at: <https://apps.ecmwf.int/dataset/data/interim-full-daily>, 2017.
- Gillet, N. P., Zwiers Francis W., Weaver Andrew J., and Stott Peter A.: Detection of human influence on sea-level pressure, *Nature*, 422, 292, <https://doi.org/10.1038/nature01487>, 2003.
- Graversen, R. G.: Do changes in the midlatitude circulation have any impact on the Arctic surface air temperature trend?, *Journal of climate*, 19, 5422–5438, <https://doi.org/10.1175/JCLI3906.1>, 2006.
- Hazeleger, W., Wang, X., Severijns, C., Ștefănescu, S., Bintanja, R., Sterl, A., Wyser, K., Semmler, T., Yang, S., van den Hurk, B., van Noije, T., van der Linden, E., and van der Wiel, K.: EC-Earth V2.2: description and validation of a new seamless earth system prediction model, *Climate Dynamics*, 39, 2611–2629, <https://doi.org/10.1007/s00382-011-1228-5>, 2012.
- Higgins, E. M. and Cassano, J. J.: Impacts of reduced sea ice on winter Arctic atmospheric circulation, precipitation, and temperature, *Journal of Geophysical Research: Atmospheres*, 114, <https://doi.org/10.1029/2009JD011884>, 2009.
- Kohonen, T.: The self-organizing map, *Neurocomputing*, 21, 1–6, [https://doi.org/10.1016/S0925-2312\(98\)00030-7](https://doi.org/10.1016/S0925-2312(98)00030-7), 1998.
- Linden, E. C., Bintanja, R., and Hazeleger, W.: Arctic decadal variability in a warming world, *Journal of Geophysical Research: Atmospheres*, 122, 5677–5696, <https://doi.org/10.1002/2016JD026058>, 2017.
- Liu, Y. and Weisberg, R. H.: A review of Self-Organizing Map applications in meteorology and oceanography, *InTech*, <https://doi.org/10.5772/13146>, 2011.
- Liu, Y., Weisberg, R. H., and Mooers, C. N. K.: Performance evaluation of the self-organizing map for feature extraction, *Journal of Geophysical Research: Oceans*, 111, <https://doi.org/10.1029/2005JC003117>, 2006.
- Lynch, A. H., Serreze, M. C., Cassano, E. N., Crawford, A. D., and Stroeve, J.: Linkages between Arctic summer circulation regimes and regional sea ice anomalies, *J. Geophys. Res. Atmos.*, 121, 7868–7880, <https://doi.org/10.1002/2016JDS025164>, 2016.





- Matthes, H., Rinke, A., and Dethloff, K.: Recent changes in Arctic temperature extremes: warm and cold spells during winter and summer, *Environmental Research Letters*, 10, 114 020, <https://doi.org/10.1088/1748-9326/10/11/114020>, 2015.
- Mattingly, K. S., Ramseyer, C. A., Rosen, J. J., Mote, T. L., and Muthyala, R.: Increasing water vapor transport to the Greenland Ice Sheet revealed using self-organizing maps, *Geophys. Res. Lett.*, 43, 9250–9258, <https://doi.org/10.1002/2016GL070424>, 2016.
- 5 Messori, G., Woods, C., and Caballero, R.: On the drivers of wintertime temperature extremes in the high Arctic, *Journal of Climate*, 31, 1597–1618, <https://doi.org/10.1175/JCLI-D-17-0386.1>, 2018.
- Overland, J. E., Wood, K. R., and Wang, M.: Warm Arctic—cold continents: climate impacts of the newly open Arctic Sea, *Polar Research*, 30, 15 787, <https://doi.org/10.3402/polar.v30i0.15787>, 2011.
- Rinke, A. and Dethloff, K.: Simulated circum-Arctic climate changes by the end of the 21st century, *Global and Planetary Change*, 62,  
10 173–186, <https://doi.org/10.1016/j.gloplacha.2008.01.004>, 2008.
- Rinke, A., Maturilli, M., Graham, R. M., Matthes, H., Handorf, D., Cohen, L., Hudson, S. R., and Moore, J. C.: Extreme cyclone events in the Arctic: Wintertime variability and trends, *Environmental Research Letters*, 12, 094 006, 2017.
- Screen, J. A., Deser, C., Simmonds, I., and Tomas, R.: Atmospheric impacts of Arctic sea-ice loss, 1979–2009: separating forced change from atmospheric internal variability, *Climate Dynamics*, 43, 333–344, <https://doi.org/10.1007/s00382-013-1830-9>, 2014.
- 15 Simmons, A. J. and Paul, P.: Arctic warming in ERA-Interim and other analyses, *Quarterly Journal of the Royal Meteorological Society*, 141, 1147–1162, <https://doi.org/10.1002/qj.2422>, 2015.
- Skific, N., Francis, J. A., and Cassano, J. J.: Attribution of projected changes in atmospheric moisture transport in the Arctic: A self-organizing map perspective, *Journal of Climate*, 22, 4135–4153, <https://doi.org/10.1175/2009JCLI2645.1>, 2009.
- Stroeve, J. C., Serreze, M. C., Holland, M. M., Kay, J. E., Malanik, J., and Barrett, A. P.: The Arctic’s rapidly shrinking sea ice cover: a  
20 research synthesis, *Climatic Change*, 110, 1005–1027, <https://doi.org/10.1007/s10584-011-0101-1>, 2012.
- Vinogradova, A.: Meridional mass and energy fluxes in the vicinity of the Arctic border, *Izv. Atmos. Ocean Phys.*, 43, 281–293, <https://doi.org/10.1134/S0001433807030036>, 2007.
- Wei, T., Minghu, D., Bingyi, W., Changgui, L., and Shujie, W.: Variations in temperature-related extreme events (1975–2014) in Ny-Ålesund, Svalbard, *Atmospheric Science Letters*, 17, 102–108, <https://doi.org/10.1002/asl.632>, 2015.
- 25 Wendisch, M., Brückner, M., Burrows, J., Crewell, S., Dethloff, K., Ebell, K., Lüpkes, C., Macke, A., Notholt, J., Quaas, J., et al.: Understanding causes and effects of rapid warming in the Arctic, *EOS*, 98, <https://doi.org/10.1029/2017EO064803>, 2017.
- Witek, P., Gao, S. C., Lim, I. S., and Zhao, L.: somoclu: an efficient distributed library for self-organizing maps, *J. Stat. Softw.*, 78, 1–21, <https://doi.org/10.18637/jss.v078.i09>, 2017.
- Yoshimori, M., Abe-Ouchi, A., and Laîné, A.: The role of atmospheric heat transport and regional feedbacks in the Arctic warming at  
30 equilibrium, *Climate Dynamics*, 49, 3457–3472, <https://doi.org/10.1007/s00382-017-3523-2>, 2017.